Asian Journal of Chemistry; Vol. 33, No. 7 (2021), 1631-1637

ASIAN JOURNAL OF CHEMISTRY

https://doi.org/10.14233/ajchem.2021.23246

Ratiometric Sensing and Discrimination of Rutile and Anatase TiO_2 Nanoparticles by a Quinoline-Benzimidazole Conjugate

S. SUGUNA[1], K. VELMURUGAN[2], I. SHEEBHA[3], C. IMMANUEL DAVID[1], B. VIDHYA[3,*], J. PRABHU[1] and R. NANDHAKUMAR[1,*]

[1]Department of Applied Chemistry, Karunya Institute of Technology and Sciences (Deemed-to-be University), Karunya Nagar, Coimbatore-641114, India
[2]College of Material Science and Technology, Nanjing University of Aeronautics and Astronautics, Nanjing 211100, P.R. China
[3]Department of Applied Physics, Karunya Institute of Technology and Sciences (Deemed-to-be University), Karunya Nagar, Coimbatore-641114, India

*Corresponding authors: E-mail: vidhya@karunya.edu; nandhakumar@karunya.edu

Received: 13 April 2021; *Accepted*: 12 May 2021; *Published online*: 26 June 2021; AJC-20406

A quinoline-benzimidazole conjugate **1** has been synthesized as a potential probe to discriminate the TiO_2 anatase and rutile nanoparticles by fluorimetry. Probe **1** exhibits selective TiO_2 sensing through a photoinduced electron transfer process (PET) and the ratiometric sensing response by intramolecular charge transfer (ICT) mechanism. The binding ratio and the association constants were also calculated. The limit of detection of TiO_2 nanoparticles by probe **1** was upto micro molar concentrations.

Keywords: Chemosensor, TiO_2, Quinoline, Benzimidazole, Fluorescence, Ratiometric.

INTRODUCTION

Currently, the rapid growth and development of nanotechnology, which detrimentally affects the human health and environmental systems by manufactured nanoparticles [1,2]. Particularly, nano-sized titanium dioxide ($nTiO_2$), has potential usage in wide range of applications such as sunscreens, cosmetics, surface coatings, paints and in the environmental sanitization of soil, water and air [3-6]. Thus, the widespread usage of $nTiO_2$ could cause a hazard to the human being and bionetworking system. Almost all of the toxicity experiments of $nTiO_2$ were carried out on mice, rats and cell lines. Over exposure of $nTiO_2$ causes pulmonary inflammation, myocardial damage and hepatic injury [7-9]. In particular, anatase TiO_2 particles (10-20 nm) influenced an apoptosis, lipid peroxidation, micronuclei formation and oxidative DNA damages [10,11]. Therefore, the design and synthesis of fluorescent probes for the sensing of $nTiO_2$ is highly desirable to date.

Recently, a heterocyclic quinoline and imidazole derivatives plays a major role in pharmacological and optical fields. Those derivatives are a part of structural unit in the living systems and have a considerable attention for utilizing their fluorescence and chemiluminescence behaviours [12-15]. Nanoparticles generally quench the fluorescence *via* surface modified organic ligands and their reports are (i) rhodamine derivative by silica material, (ii) DN-BODIPY by TiO_2, (iii) phosphate-modified TiO_2 nanoparticles, (iv) tetrazine-modified TiO_2 nanoparticles, (v) phycoerythrin by TiO_2, $AuTiO_2$ and $AgTiO_2$ [16-20], *etc*. Hence, only few reports are available related to sensing of rutile and anatase phases of TiO_2 with "turn on" or "turn off" spectral responses [19,20]. Those reports have some disadvantages such as insufficient selectivity, quenching nature and an inability to discriminate rutile and anatase phases of TiO_2 separately [21-23]. Thus, development of new fluorescent probes for TiO_2 by overcoming the above mentioned problems and achieving ratiometric probes would be enviable. To the best of our knowledge, this is the first report to sense and study about the interaction of nanoparticles with quinoline-benzimidazole conjugate (**1**). The present study focuses on to discriminate the anatase and rutile phases of TiO_2 nanoparticles by probe **1** *via* ratiometric fluorescent responses. Probe **1** ratiometrically sense the rutile and anatase TiO_2 nanoparticles prepared by two different ways such as sol-gel and ball milling methodology. Probe **1** successfully discriminated the two different phases

of rutile and anatase TiO_2 nanoparticles with the influence of ratiometric emission enhancements, whereas, other metal oxides quenches the fluorescence upon interaction with quinoline-benzimidazole conjugate.

EXPERIMENTAL

Chemicals, solvents and reagents were commercially purchased with high purity from local chemical suppliers. The chemicals from Sigma-Aldrich and of analytical grade (Merck) were used without any further purification. Spectroscopic characterization techniques such as ^1H & ^{13}C NMR spectra were recorded on a Bruker 400 MHz and 100 MHz NMR spectrometer, with chemical shifts (ppm) in DMSO-d_6 and TMS used as an internal standard, respectively. LC-MS were performed on Agilent 6520 (Q-TOF). Shimadzu UV-240 spectrophotometer and Jasco FP-8200 spectrofluorometer were handled for UV-vis absorption and fluorescence measurement studies. All fluorescence spectral studies were carried out at 24 ± 1 ºC. For analysis, freshly prepared stock solutions were used (2×10^{-3} M of probe **1** in $CH_3CN:H_2O$, 1:1 v/v, HEPES = 50 mM, pH = 7.4-7.6). The solutions of metal oxides such as TiO_2-anatase, TiO_2-rutile, TiO_2 rutile-anatase mixture, NiO, MgO, ZnO, WO_3, Fe_2O_3, V_2O_5, $SnWO_4$, TiO_2-CNT and CuO were prepared by sol-gel and ball milling methods.

Synthesis of 3-(1*H*-benzo[*d*]imidazol-2-yl)quinolin-2-ol (1): Based on reported literature, we synthesized this receptor **1** [24]. In brief, 2-hydroxyquinoline-3-carbaldehyde (0.50 g, 2.89 mmol) was dissolved in ethanol (20 mL) and added into the solution of *o*-phenylenediamine (0.34 g, 3.17 mmol) in the presence of triethylamine. The above mixture was stirred and refluxed for 5 h. The resulting precipitate was filtered and recrystallized from chloroform to afford probe **1**. Yellow solid (yield: 80%). m.p.: 252 ºC; ^1H NMR (400 MHz, DMSO-d_6) δ ppm: 12.65 (s, 1H), 12.47 (s, 1H), 9.11 (s, 1H), 7.95 (d, 1H), 7.73-7.59 (m, 3H), 7.43 (d, 1H), 7.29 (t, 1H), 7.23-7.18 (m, 2H); ^{13}C NMR (100 MHz, DMSO-d_6) δ ppm: 113.2, 115.7, 118.7, 119.6, 120.4, 122.3, 122.7, 123.1, 129.5, 132, 134.9, 139.1, 139.5, 143.2, 148.1, 161.2. Elemental analysis of $C_{16}H_{11}N_3O$; calcd. (found) %; C, 73.55 (73.48); H, 4.24 (4.21); N, 16.08 (16.02). LC-MS: *m/z* 262 $[M^+ + H]^+$.

Preparation of TiO_2 by ball milling and sol-gel method

Ball milling method: Anatase, rutile and mixed phase TiO_2 were prepared by changing the milling time at a fixed rpm using a Fritsch premium line 6 Planetary Micro Ball Mill. The details of preparation and structural studies are reported in detail in previous work [25].

Sol-gel method: The sol-gel synthesized TiO_2 was obtained from titanium isopropoxide (TTIP), which was dissolved in 2-propanol in the ratio 1:4. This solution was added into a mixture of H_2O and 2-propanol of ratio 1:1 dropwise amidst vigorous stirring. The pH of the mixture was adjusted using ammonia. This mixture was kept under continuous stirring for 1 h to form the gel. This was dried for several hours at 105 ºC, which formed a crystal block. Then the dried gel was sintered at 500, 700 and 800 ºC for 1 h each to obtain the desired TiO_2 particles in different phases.

RESULTS AND DISCUSSION

Structural studies of TiO_2 prepared by ball milling and sol-gel method: The XRD pattern of TiO_2 sample prepared by sol-gel method, after annealing at 500 ºC shows the peaks corresponding to anatase phase, which was confirmed by the JCPDS data #894921 and #020494 (Fig. 1a). As the annealing temperature increased to 700 ºC, the XRD pattern showed a mixture of both anatase and rutile phase. Further annealing to a temperature of 800 ºC gives the pure tetragonal structured rutile crystalline phase. TiO_2 prepared by sol-gel method was found to have better crystallinity than ball milled TiO_2.

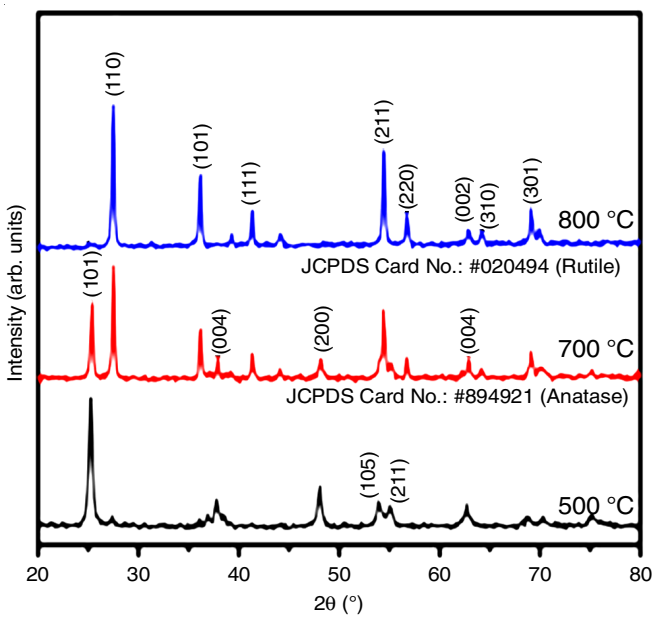

Fig. 1a. X-ray diffraction pattern of TiO_2 prepared by sol-gel method

Fig. 1b shows the X-ray diffraction pattern of the ball milled samples. The sample milled at 400 rpm, remains in anatase phase. With the increase in milling time, a mixed anatase and rutile phase is observed for the sample milled at 700 rpm. Further increase in milling time resulted in the formation of rutile phase. The obtained data matches well with the standard JCPDS data #894921 and #020494. The crystallinity of the sample was found to be deteriorated with the increase in milling time which is evident from the broadening of XRD peaks.

The average crystallite size of the prepared TiO_2 particles were calculated using Debye- Scherrer formula (eqn. 1) and listed in Table-1.

$$D = \frac{0.9\lambda}{\beta \cos\theta} \quad (1)$$

From the calculated values, it is observed that though phase change is observed in both top-down (ball milling) and bottom-up (sol gel) method, there is a difference in crystallite size. The crystallite size decreases with the increase in milling time whereas there is an increase in crystallite size with the increase in sintering temperature in sol gel method.

Sensing ability of conjugate 1: The metal oxide sensing capability of conjugate **1** was methodically carried out for diffe-

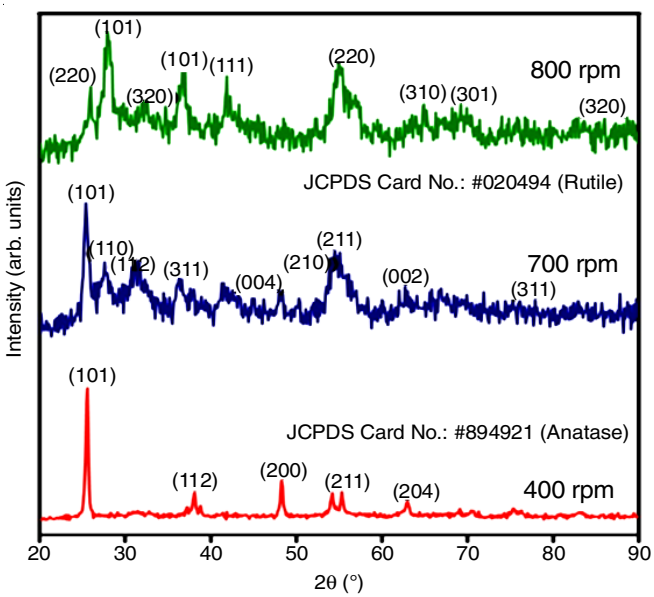

Fig. 1b. X-ray diffraction pattern of TiO_2 prepared by ball milling method at different rpm

TABLE-1
AVERAGE CRYSTALLITE SIZE OF THE PREPARED TiO_2 PARTICLES

Preparation method	Sample	Phase	Crystallite size (Å)
Ball milling	450 rpm	Anatase	23
	700 rpm	Anatase and rutile (mixed phase)	14
	850 rpm	Rutile	7
Sol gel	500 °C	Anatase	19
	700 °C	Anatase and rutile (mixed phase)	26
	800 °C	Rutile	28

rent metal oxides using the fluorescence technique in CH_3CN:H_2O (1:1 (v/v), HEPES = 50 mM, pH = 7.4-7.6) solution (Fig. 2). Before the experiment, the excitation wavelength of probe was fixed from the UV-visible spectra. The emission spectrum of conjugate **1** (4 μM) displayed a weak and single emission band at 425 nm due to intramolecular photo induced electron transfer (PET) process in hetero atoms containing benzimidazole and quinoline scaffolds.

Addition of anatase TiO_2 and rutile TiO_2 nanoparticles (100 equiv.) prepared by two different methods such as sol-gel and ball milling methods could cause a ratiometric emission enhancement with the emission maxima at 408 nm were observed in both cases (Fig. 2). In contrast, addition of identical concentration of other metal oxides (100 equiv.) prepared by sol-gel and ball milling methods such as TiO_2-rutile and anatase mixture, NiO, MgO, ZnO, WO_3, Fe_2O_3, V_2O_5, $SnWO_4$, TiO_2-CNT and CuO to conjugate **1**, quenches the fluorescence. These discriminating capabilities of probe conjugate **1** revealed that the selective ratiometric emission enhancement towards TiO_2-anatase and TiO_2-rutile nanoparticles are probably by dual pathways such as (i) inhibiting the photoinduced electron transfer process due to the presence of hetero atoms containing quinoline-benzimidazole conjugate and (ii) by intramolecular charge transfer (ICT) process between quinoline and benzimidazole ring [26-30].

To investigate its specificity and sensitivity, the anti-interfering property were studied with all other metal oxides in the presence of TiO_2-anatase and rutile nanoparticles on conjugate **1** was studied, separately. Fig. 3 shows the strong fluorescence enhancement in the presence of TiO_2-anatase and rutile nanoparticles to conjugate **1**, which are not interfered by the addition of other metal oxides. These findings revealed that conjugate **1** selectively discriminates TiO_2-anatase and rutile nanoparticles and there was no influence of other metal oxides in the detection of TiO_2-anatase and rutile phases. This is the first report where the probe conjugate **1** is able to discriminate TiO_2-anatase and rutile phases by inhibition of PET process leading to ICT mechanism between quinoline-benzimidazole conjugates. This determines that probe conjugate **1** strongly binds with TiO_2-anatase and rutile nanoparticles prepared by two different methodologies such as ball milling and sol-gel method.

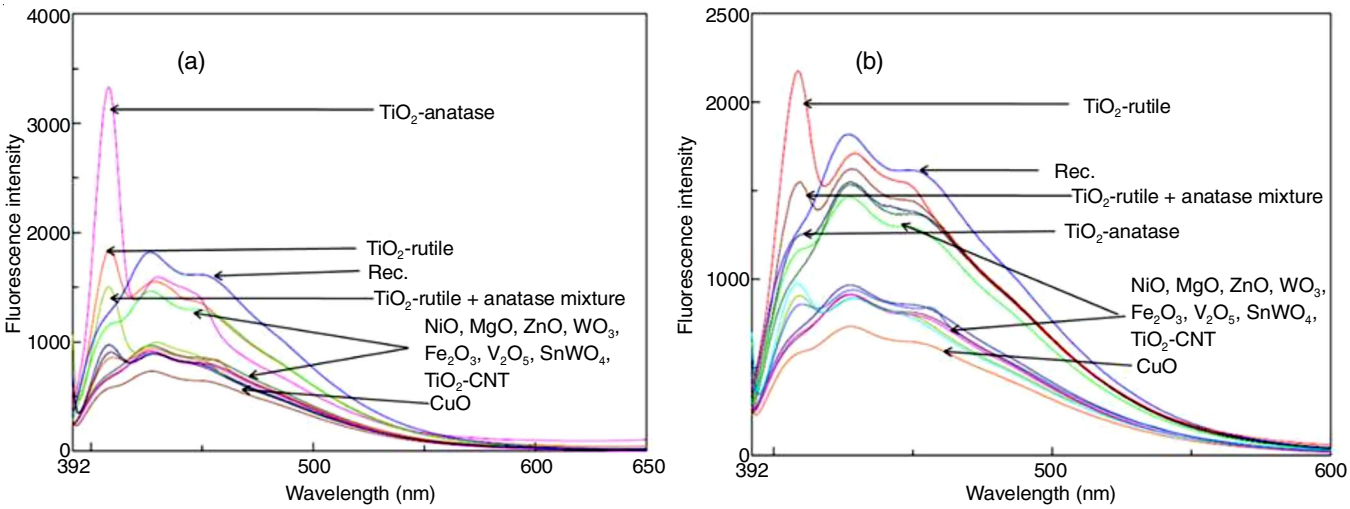

Fig. 2. Fluorescence emission changes of conjugate **1** (4×10^{-6} M) in CH_3CN:H_2O (1:1 v/v, HEPES = 50 mM, pH = 7.4-7.6) solution in the presence of different metal oxides (100 equiv. of each, excited at 380 nm) prepared by (a) ball milling and (b) solgel method

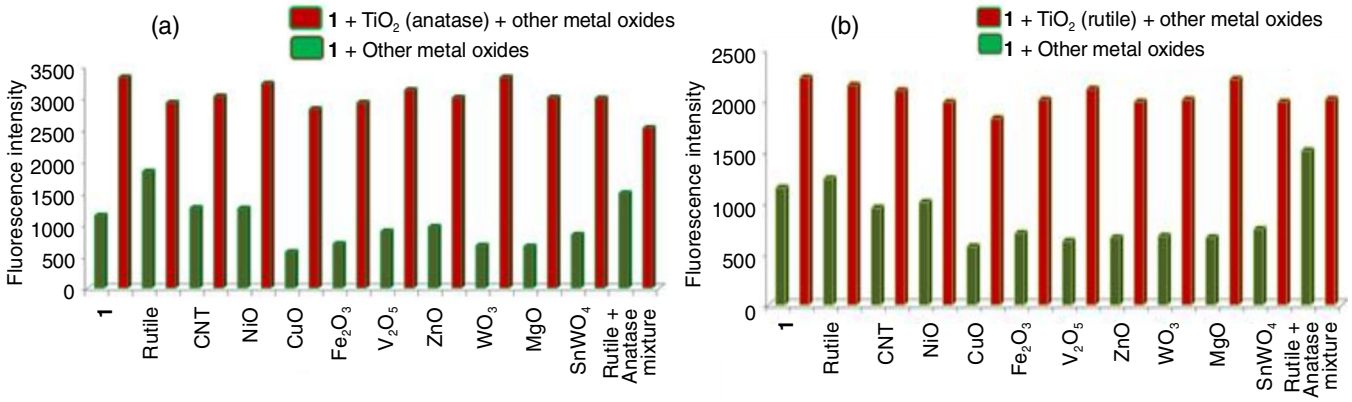

Fig. 3. Fluorescence emission changes of conjugate **1** (4×10^{-6} M) $CH_3CN:H_2O$ (1:1 v/v, HEPES = 50 mM, pH = 7.4-7.6) solution in the presence of various metal oxides upon addition of (a) TiO_2-anatase (100 equiv. of each) (b) TiO_2-rutile (100 equiv. of each)

Spectroscopic titration of conjugate 1 to TiO_2-anatase and TiO_2-rutile: Fluorescence titration spectrum of conjugate **1** with the gradual loading of TiO_2-anatase and TiO_2-rutile (0 to 16 equiv) were added, individually (Fig. 4). Stepwise, gradual addition of TiO_2-anatase and rutile to conjugate **1** lead to a ratiometric emission enhancements with isoemissive point at 415 nm and becomes saturated when 12 and 16 equiv of TiO_2-anatase and rutile nanoparticles were added respectively. This ratiometric emission enhancement indicates that the adsorption of quinoline-benzimidazole derivative on TiO_2 anatase and rutile surfaces led to effective ICT process. The binding stoichiometry of TiO_2 rutile and anatase with conjugate **1** was determined by Job's plot method. Fig 5 displays the maximum emission were found at 0.72 mole fraction, which reveals that 1:2 binding stoichiometry between conjugate **1** with each TiO_2 rutile and anatase nanoparticles separately [31,32].

Furthermore, the 1:2 binding ratio was evaluated with the help of fluorescence titration data of TiO_2 rutile and anatase phases with conjugate **1** was plotted by $\log (I - I_0)/(I_\infty - I)$ *versus* $\log C_G$ (Fig. 6). Based on the non-linear fitting of the titration curve [33,34], the association constant (K_a) of **1**+TiO_2 anatase and **1**+TiO_2 rutile were computed to be 6.34×10^4 M^{-2} and 5.179×10^4 M^{-2}, respectively, indicating that each quinoline-benzimidazole molecule was bound to two TiO_2 molecules. The detection limit of conjugate **1** was calculated to be 13.72 μM (TiO_2 anatase) and 13.62 μM (TiO_2 rutile) by using the formula 3δ/S [35,36].

pH and time response of conjugate 1: For a potent chemosensor, the sensing efficiency at the physiological pH is very crucial. Hence, the pH effect on conjugate **1** in the presence and absence of TiO_2 rutile and anatase in $CH_3CN:H_2O$ (1:1 v/v) was experimented (Fig. 7). The fluorescence intensity of conjugate **1** was steady and not affected by various pH ranges. Treatment of TiO_2 rutile and anatase nanoparticles to conjugate **1**, ratiometric fluorescence was observed between the pH 6-9. However, when the pH is less than 6 or greater than 9, decreases the fluorescence intensity and isosbestic point was not observed in those ranges. Therefore, above result reveals that conjugate **1** can be used for the environmental, clinical and biological applications at a physiological pH. Furthermore, the rapid time response of conjugate **1** for the recognition of TiO_2 anatase and rutile in $CH_3CN:H_2O$ (1:1 v/v, HEPES = 50 mM, pH = 7.4-7.6) was achieved (Fig. 8). It results that probe conjugate **1** can bind with 100 equiv of TiO_2 anatase and rutile nanoparticles in almost 2 min to attain the maximum intensity without any changes.

FT-IR studies: Additionally, the nature of binding interaction between the small heterocyclic molecule containing C=N & amide 'O' groups with TiO_2 anatase and rutile nanoparticles

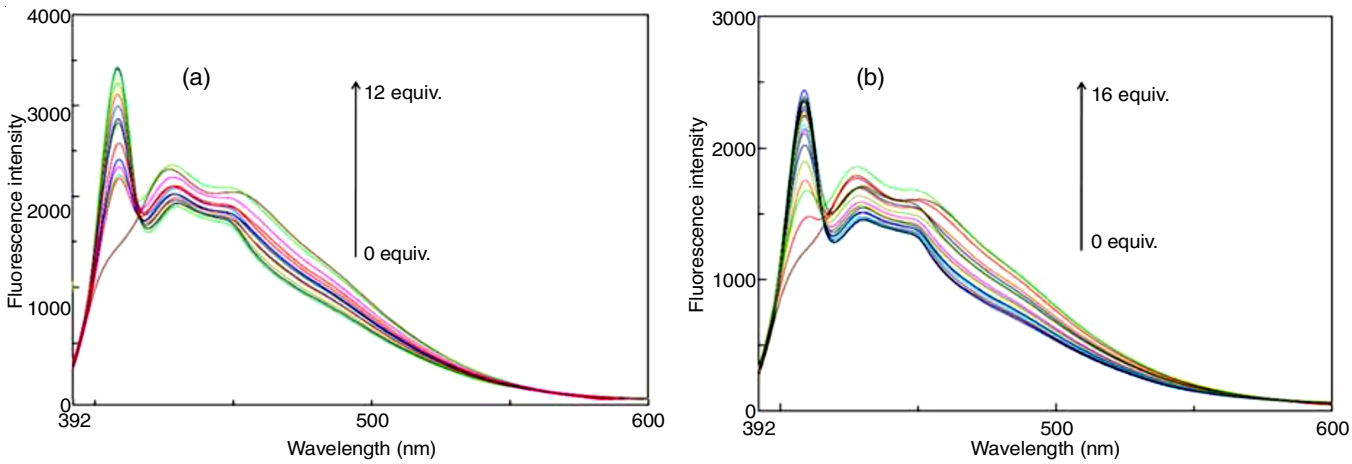

Fig. 4. Changes in fluorescence spectrum of conjugate **1** (4×10^{-6} M) $CH_3CN:H_2O$ solution (1:1 v/v, HEPES = 50 mM, pH = 7.4-7.6) upon addition of different amount of (a) TiO_2 (anatase) (0-12 equiv.) by sol-gel method (b) TiO_2 (rutile) by ball milling method

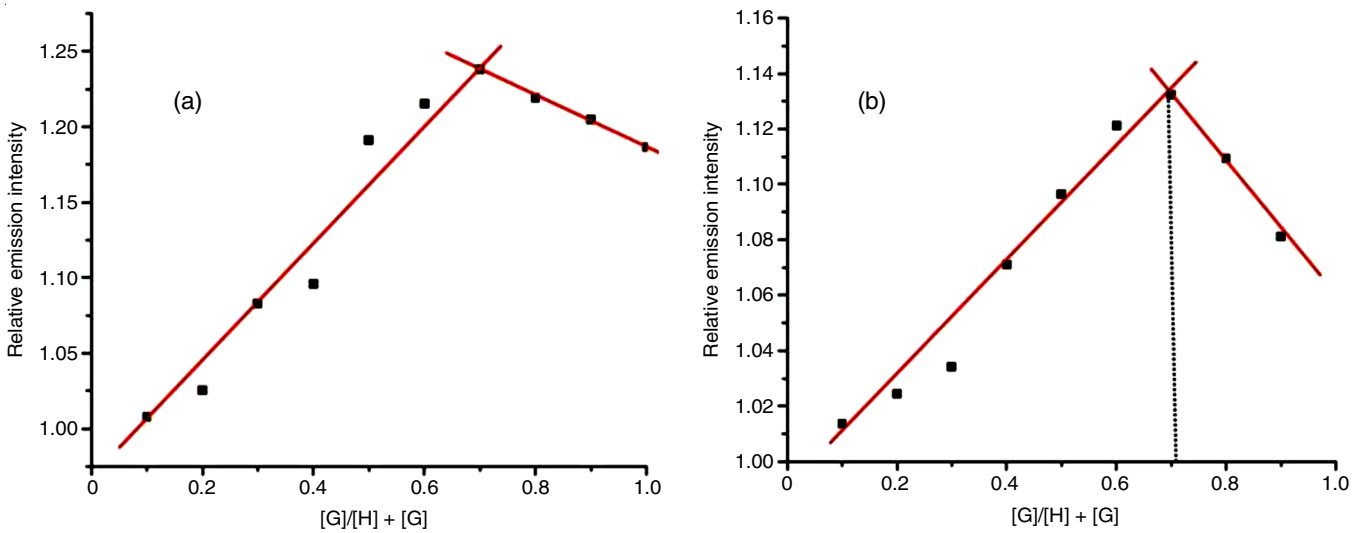

Fig. 5. Job's plot for probe **1** with (a) TiO_2 (anatase) and (b) TiO_2 (rutile) in $CH_3CN:H_2O$ (1:1 v/v, HEPES = 50 mM, pH = 7.4-7.6) solution

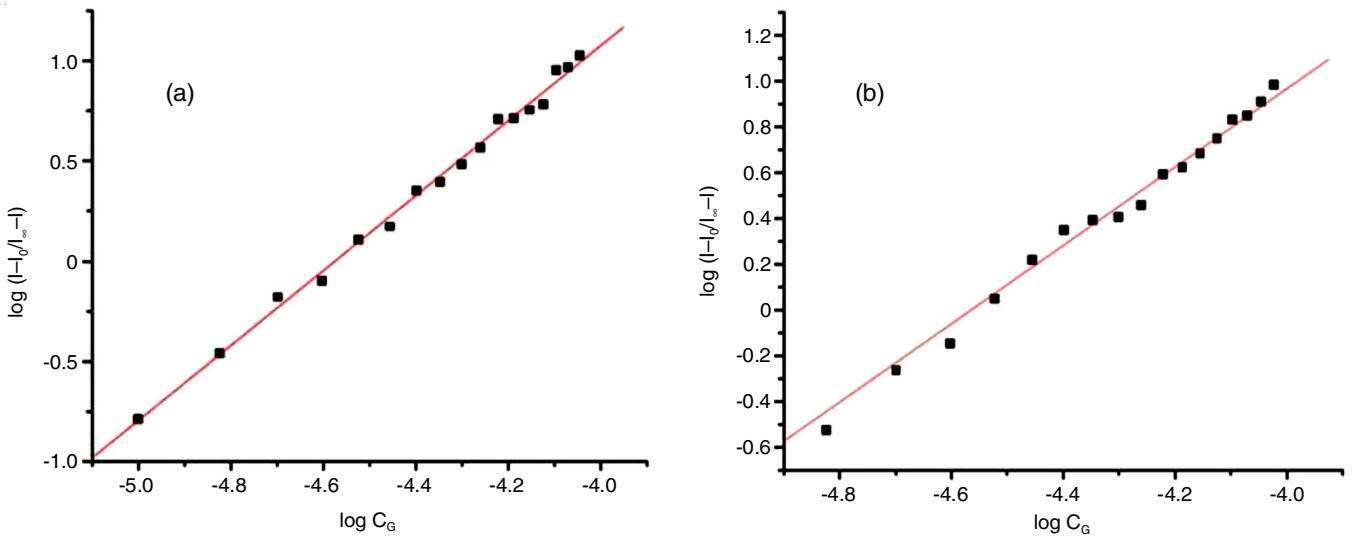

Fig. 6. Benesi-Hildebrand plot of conjugate **1**, assuming 1:2 stoichiometry for (a) conjugate **1** with TiO_2 (anatase) and (b) **1** with TiO_2 (rutile) nanoparticles

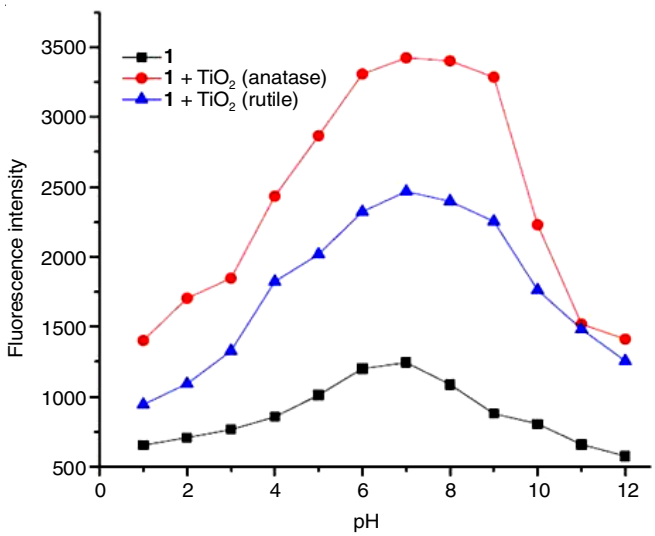

Fig. 7. Effect of pH on conjugate **1**, **1** + TiO_2 (anatase) and **1** + TiO_2 (rutile) in $CH_3CN:H_2O$ (1:1 v/v) solution

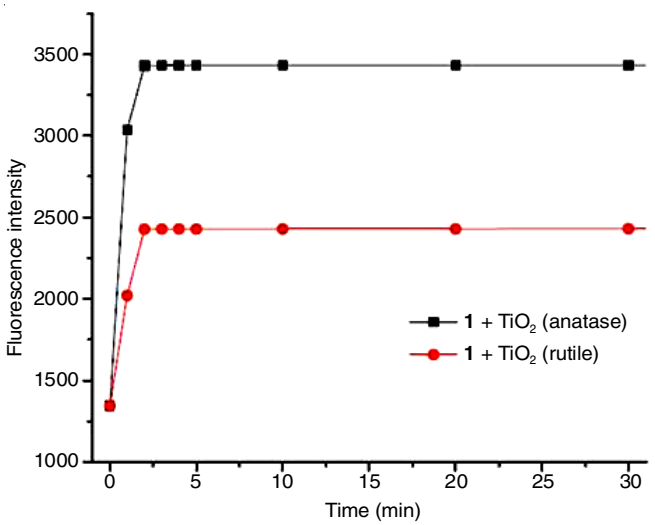

Fig. 8. Effective time response of conjugate **1**, **1** + TiO_2 (anatase) and **1** + TiO_2 (rutile) in $CH_3CN:H_2O$ (1:1 v/v, HEPES = 50 mM, pH = 7.4-7.6) solution

is further confirmed using IR spectrum in aqueous media (Fig. 9). IR spectrum of conjugate **1**, a reference compound measured in a $CH_3CN:H_2O$ mixture (1:1 v/v, pH=7.4-7.6) shows absorption bands at 1662 cm^{-1} (strong) and 2366 cm^{-1} (weak) assigned to the C=N and amide 'O' vibrational stretching for quinoline-benzimidazole moiety [37,38]. Addition of TiO_2 rutile and anatase to the solution of conjugate **1**, C=N and amide 'O' absorption bands downward shifted to 1656, 2361 and 2355 cm^{-1}, which is assigned to the C=N & amide 'O' band confirms the quinoline-benzimidazole derivative is adsorbed on the surface of anatase and rutile TiO_2 nanoparticles as shown in **Scheme-I**.

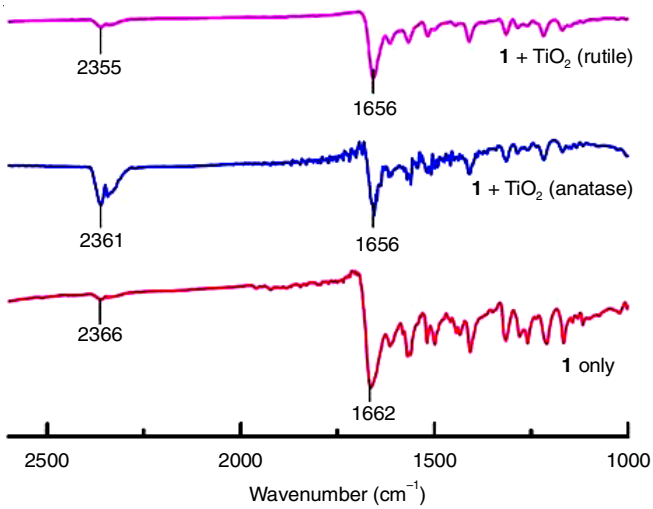

Fig. 9. IR spectrum of conjugate **1** only, **1** + TiO_2 (anatase) and **1** + TiO_2 (rutile)

Morphology studies: Scanning electron microscopy (SEM) of quinoline-imidazole derivative (**1**) adsorbed on TiO_2 anatase and rutile nanoparticles are shown in Fig. 10. The SEM results of free receptor **1** shows flake like morphology and after adsorption with TiO_2 the flake morphology modified to rod like structure and their size is also decreased. In addition, modified rod like structure of conjugate **1** is surrounded by TiO_2 rutile and anatase nanoparticles, which is clearly observed in Fig. 10b-c. On the basis of above results, the adsorption behaviour of the probe conjugate **1** on TiO_2 rutile and anatase nanocrystalline surfaces were confirmed undoubtedly.

Proposed mechanism: The proposed signaling mechanism of conjugate **1** was based upon the inhibition of PET followed

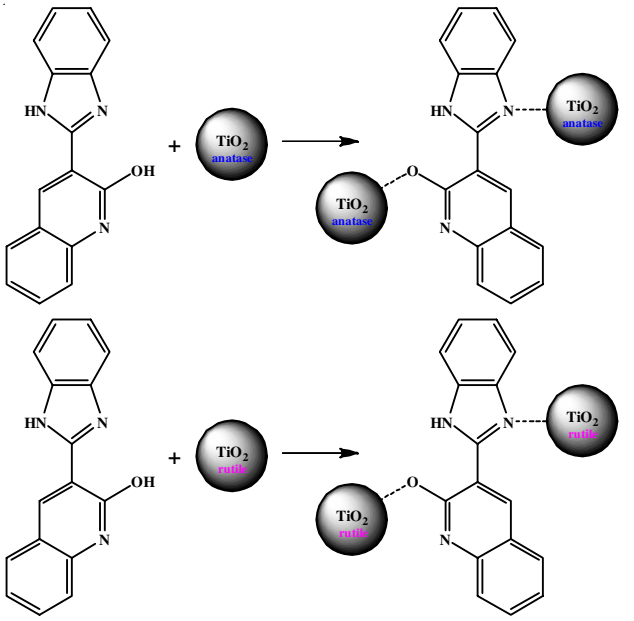

Scheme-I: Proposed signaling mode of conjugate **1** with TiO_2 anatase and rutile nanoparticles

by ratiometric response was observed with the help of ICT process. Free receptor **1** exhibits a weak fluorescence owing to the photoinduced electron transfer process from imidazole moiety possess hetero atoms with lone pair of electrons makes non-radiative relaxation process in the excited state molecule. Addition of TiO_2 anatase and rutile nanoparticles influences the ratiometric signals through chelation forming benzimidazole and quinoline (imine 'nitrogen' and the amide 'carbonyl oxygen') moieties, which would lead to ratiometric signals. Thus, the probe conjugate **1** serves a selective TiO_2 anatase and rutile nanoparticle sensor by the ratiometric fluorescent signals.

Conclusion

In conclusion, the prepared probe conjugating quinoline and benzimidazole scaffolds (conjugate **1**), which potentially detect the TiO_2 anatase and rutile nanoparticles by fluorimetrically. The TiO_2 anatase and rutile chelating behaviour encompassing the benzimidazole nitrogen and the quinoline carbonyl confirmed selective TiO_2 binding, which causes an inhibition of non-radiative decay pathways like PET process and ratiometric sensing response by ICT mechanism of probe conjugate **1**. The probe conjugate **1** can be potentially applied to detect

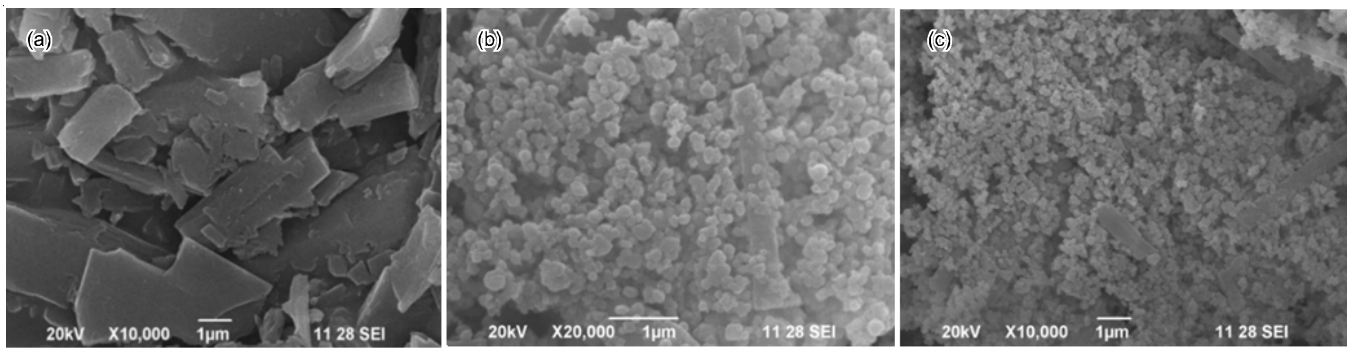

Fig. 10. (a) SEM images of free receptor **1** only (b) **1** adsorbed in anatase TiO_2 nanoparticle. (c) **1** adsorbed in rutile TiO_2 nanoparticle

TiO_2 anatase and rutile nanoparticles downs to micromolar concentrations in environmental and biological samples.

ACKNOWLEDGEMENTS

This work is supported by the SERB-EMR grant by the DST (Sanction No. SERB-EMR/2016/005692). Gandhigram Rural Institute (supported by DST-FIST) supported the spectral details for this work. one of the authors, S. Suguna is thankful to Karunya Institute of Technology and Sciences for providing the financial support through Evangeline Dhinakaran Doctoral Fellowship.

CONFLICT OF INTEREST

The authors declare that there is no conflict of interests regarding the publication of this article.

REFERENCES

1. R.F. Service, *Science*, **310**, 1609 (2005); https://doi.org/10.1126/science.310.5754.1609
2. A. Nel, T. Xia, L. Madler and N. Li, *Science*, **311**, 622 (2006); https://doi.org/10.1126/science.1114397
3. J. Fisher and T. Egerton, Kirk-Othmer Encyclopedia of Chemical Technology, John Wiley: New York (2001).
4. T. Kaida, K. Kobayashi, M. Adachi and F. Suzuki, *J. Cosmet. Sci.*, **55**, 219 (2004).
5. C.R. Esterkin, A.C. Negro, O.M. Alfano and A.E. Cassano, *AIChE J.*, **51**, 2298 (2005); https://doi.org/10.1002/aic.10472
6. H. Choi, E. Stathatos and D.D. Dionysiou, *Appl. Catal. B*, **63**, 60 (2006); https://doi.org/10.1016/j.apcatb.2005.09.012
7. D.B. Warheit, T.R. Webb, K.L. Reed, S. Frerichs and C.M. Sayes, *Toxicology*, **230**, 90 (2007); https://doi.org/10.1016/j.tox.2006.11.002
8. D.B. Warheit, T.R. Webb, C.M. Sayes, V.L. Colvin and K.L. Reed, *Toxicol. Sci.*, **91**, 227 (2006); https://doi.org/10.1093/toxsci/kfj140
9. D.B. Warheit, W.J. Brock, W.J. Lee, K.P. Webb and K.L. Reed, *Toxicol. Sci.*, **88**, 514 (2005); https://doi.org/10.1093/toxsci/kfi331
10. J. Gurr, A.S.S. Wang, C. Chen and K. Jan, *Toxicology*, **213**, 66 (2005); https://doi.org/10.1016/j.tox.2005.05.007
11. Q. Rahman, M. Lohani, E. Dopp, H. Pemsel, L. Jonas, D.G. Weiss and D. Schiffmann, *Environ. Health Perspect.*, **110**, 797 (2002); https://doi.org/10.1289/ehp.02110797
12. D.W. Nebert and F.J. Gonzalez, *Annu. Rev. Biochem.*, **56**, 945 (1987); https://doi.org/10.1146/annurev.bi.56.070187.004501
13. K. Nakashima, A. Kaddoumi, Y. Ishida, T. Itoh and K. Taki, *Biomed. Chromatogr.*, **17**, 471 (2003); https://doi.org/10.1002/bmc.278
14. Q. Feng, J. Wu, G. Chen, F. Cui, T. Kim and J. Kim, *J. Biomed. Mater. Res.*, **52**, 662 (2000); https://doi.org/10.1002/1097-4636(20001215)52:4<662::AID-JBM10>3.0.CO;2-3
15. R. Nandhakumar, T. Suresh, A.L.C. Jude, V. Rajesh kannan and P.S. Mohan, *Eur. J. Med. Chem.*, **42**, 1128 (2007); https://doi.org/10.1016/j.ejmech.2007.01.004
16. X. Chen, T. Pradhan, F. Wang, J. S. Kim and J. Yoon, *Chem. Rev.*, **112**, 1910 (2012); https://doi.org/10.1021/cr200201z
17. T. Tachikawa, N. Wang, S. Yamashita, S.-C. Cui and T. Majima, *Angew. Chem. Int. Ed.*, **49**, 8593 (2010); https://doi.org/10.1002/anie.201004976
18. H.-P. Wu, T.-L. Cheng and W.-L. Tseng, *Langmuir*, **23**, 7880 (2007); https://doi.org/10.1021/la700555y
19. S. Seo, C. Allain, J. Na, S. Kim, X. Yang, C. Park, J. Malinge, P. Audebert and E. Kim, *Nanoscale*, **5**, 7321 (2013); https://doi.org/10.1039/c3nr01648j
20. A. Kathiravan, M. Chandramohan, R. Renganathan and S. Sekar, *Spectrochimica Acta A Mol. Biomol. Spectrosc.*, **72**, 496 (2009); https://doi.org/10.1016/j.saa.2008.10.021
21. K.T. Thurn, T. Paunesku, A.G. Wu, E.M.B. Brown, B. Lai, S. Vogt, J. Maser, M. Aslam, V. Dravid, R. Bergan and G.E. Woloschak, *Small*, **5**, 1318 (2009); https://doi.org/10.1002/smll.200801458
22. I. Martini, J.H. Hodak and G.V. Hartland, *J. Phys. Chem. B*, **102**, 9508 (1998); https://doi.org/10.1021/jp972925f
23. C. Karunakaran, J. Jayabharathi, K. Jayamoorthy and K. Brindha Devi, *Sens. Actuators B Chem.*, **168**, 263 (2012); https://doi.org/10.1016/j.snb.2012.04.021
24. K. Velmurugan, A. Raman, D. Don, L. Tang, S. Easwaramoorthi and R. Nandhakumar, *RSC Adv.*, **5**, 44463 (2015); https://doi.org/10.1039/C5RA04523A
25. B. Vidhya and A. Ford, *Nanosci. Nanotechnol. Lett.*, **5**, 980 (2013); https://doi.org/10.1166/nnl.2013.1663
26. G. Ramakrishna and H.N. Ghosh, *J. Phys. Chem. B*, **105**, 7000 (2001); https://doi.org/10.1021/jp011291g
27. F. Wang, R. Nandhakumar, J.H. Moon, K.M. Kim, J.Y. Lee and J. Yoon, *Inorg. Chem.*, **50**, 2240 (2011); https://doi.org/10.1021/ic1018967
28. J. Prabhu, K. Velmurugan, A. Raman, N. Duraipandy, S. Easwaramoorthi, M.S. Kiran and R. Nandhakumar, *Sens. Actuators B Chem.*, **238**, 306 (2017); https://doi.org/10.1016/j.snb.2016.07.018
29. D. Derin, K. Velmurugan, J. Prabhu, N. Bhuvanesh, A. Thamilselvan and R. Nandhakumar, *Spectrochim. Acta A Mol. Biomol. Spectrosc.*, **174**, 62 (2016); https://doi.org/10.1016/j.saa.2016.11.021
30. K. Velmurugan, S. Santhoshkumar, M. Saranya, R. Nandhakumar and S. Suresh, *Luminescence*, **31**, 722 (2016); https://doi.org/10.1002/bio.3016
31. J. Prabhu, K. Velmurugan, Q. Zhang, S. Radhakrishnan, R. Nandhakumar and L. Tang, *J. Photochem. Photobiol. Chem.*, **337**, 6 (2017); https://doi.org/10.1016/j.jphotochem.2017.01.006
32. K. Velmurugan, A. Thamilselvan, R. Antony, V.R. Kannan, L. Tang and R. Nandhakumar, *J. Photochem. Photobiol. Chem.*, **333**, 130 (2017); https://doi.org/10.1016/j.jphotochem.2016.10.025
33. S. Santhoshkumar, K. Velmurugan, J. Prabhu, G. Radhakrishnan and R. Nandhakumar, *Inorg. Chim. Acta*, **439**, 1 (2016); https://doi.org/10.1016/j.ica.2015.09.030
34. K. Velmurugan and R. Nandhakumar, *J. Lumin.*, **162**, 8 (2015); https://doi.org/10.1016/j.jlumin.2015.01.039
35. J. Prabhu, K. Velmurugan and R. Nandhakumar, *Spectrochim. Acta A Mol. Biomol. Spectrosc.*, **144**, 23 (2015); https://doi.org/10.1016/j.saa.2015.02.028
36. K. Velmurugan, S. Mathankumar, S. Santoshkumar, S. Amudha and R. Nandhakumar, *Spectrochim. Acta A Mol. Biomol. Spectrosc.*, **139**, 119 (2015); https://doi.org/10.1016/j.saa.2014.11.103
37. K. Velmurugan, J. Prabhu, L. Tang, T. Chidambaram, S. Radhakrishnan, M. Noel and R. Nandhakumar, *Anal. Methods*, **6**, 2883 (2014); https://doi.org/10.1039/C3AY42139B
38. T. Molotsky and D. Huppert, *J. Phys. Chem. A*, **107**, 8449 (2003); https://doi.org/10.1021/jp034760i